This is an open access article published under a Creative Commons Attribution (CC-BY) License, which permits unrestricted use, distribution and reproduction in any medium, provided the author and source are cited.

analytical chemistry

Article

pubs.acs.org/ac

Dual Recognition Element Lateral Flow Assay Toward Multiplex Strain Specific Influenza Virus Detection

Thao T. Le,[†] Pengxiang Chang,[‡] Donald J. Benton,[§] John W. McCauley,[§] Munir Iqbal,[‡] and Anthony E. G. Cass*[,†]

[†]Department of Chemistry, Imperial College London, London SW7 2AZ, U.K.

[‡]Avian Viral Diseases Program, Pirbright Institute, Woking GU24 0NF, U.K.

[§]Worldwide Influenza Centre, Francis Crick Institute, London NW1 1AT, U.K.

Supporting Information

ABSTRACT: Different influenza virus strains have caused a number of recent outbreaks killing scores of people and causing significant losses in animal farming. Simple, rapid, sensitive, and specific detection of particular strains, such as a pandemic strain versus a previous seasonal influenza, plays a crucial role in the monitoring, controlling, and management of outbreaks. In this paper we describe a dual recognition element lateral flow assay (DRELFA) which pairs a nucleic acid aptamer with an antibody for use as a point-of-care platform which can detect particular strains of interest. The combination is used to overcome the individual limitations of antibodies' cross-reactivity and aptamers' slow binding kinetics. In the detection of influenza viruses, we show that DRELFA can discriminate a particular virus strain against others of the same subtype or common respiratory diseases while still exhibiting fast binding kinetic of the antibody-based lateral flow assay (LFA). The improvement in specificity that DRELFA exhibits is an advantage over the currently available antibody-based LFA systems for influenza viruses, which offer discrimination between influenza virus types and subtypes. Using quantitative real-time PCR (qRT-PCR), it showed that the DRELFA is very effective in localizing the analyte to the test line (consistently over 90%) and this is crucial for the sensitivity of the device. In addition, color intensities of the test lines showed a good correlation between the DRELFA and the qRT-PCR over a 50-fold concentration range. Finally, lateral flow strips with a streptavidin capture test line and an anti-antibody control line are universally applicable to specific detection of a wide range of different analytes.

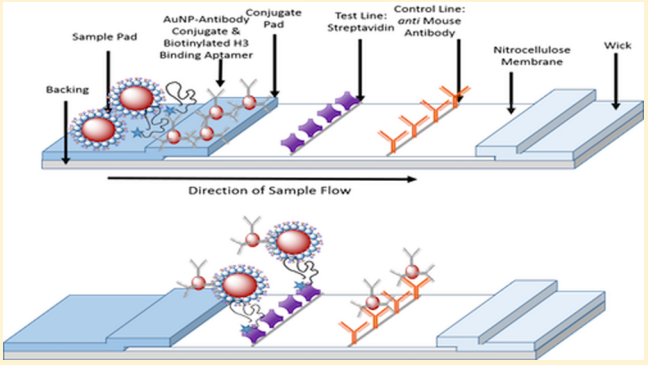

Over the years, influenza virus pandemics and outbreaks have resulted in high morbidity and mortality in both people and animals. The most deadly pandemic of modern times was the "Spanish flu" 1918-19 a H1N1 strain which caused tens of millions of deaths worldwide.[1] Other pandemics of the 20th century that caused hundreds of thousands of deaths were the "Asian flu" 1957-58 a H2N2 strain and the "Hong Kong flu" 1968-69 a H3N2 strain.[2] This century the 2009 "swine flu" pandemic infected tens of millions of people, with tens of thousands of lab-confirmed deaths.[3] Outbreaks of H5N1 strains has resulted in mass culling of millions of farmed birds,[4,5] and according to WHO's January 2017 report,[6] 856 cases of zoonotic human infection were reported, of which 452 were fatal. Diagnosis of influenza using PCR and virus culture assays are highly sensitive and specific methods that have been used as standards, with the former allowing identification of specific strains and with a detection limit of tens of viral RNA copies.[7,8] These methods are, however, laboratory-based and therefore are unable to meet the need for field diagnostic tests during a pandemic outbreak. Therefore, methods for detection of viruses that meet the WHO ASSURED criteria[9] play a crucial role not only in diagnosis during a pandemic but also in control and management of less serious outbreaks.

Point of care immunoassays are built primarily around the lateral flow assay (LFA) format, typically employing antibodies with visual detection of the endpoint immune complex formation through the use of a nanoparticle label.[10,11] Antibodies have been well established for several decades as a class of recognition molecules and used for many applications due to their high binding affinity and fast association kinetics. These characteristics mean that antibodies have been used in many diagnostic tests both laboratory-based, e.g., ELISAs[12,13] and in decentralized environments, e.g., LFA.[14]

Another notable class of recognition molecules is that of aptamers. Since the first aptamers were reported in 1990,[15,16] hundreds have been selected for both diagnostic and therapeutic applications.[17,18] Aptamers have frequently been

Received: March 28, 2017
Accepted: May 30, 2017
Published: May 30, 2017

 © 2017 American Chemical Society

DOI: 10.1021/acs.analchem.7b01149
Anal. Chem. 2017, 89, 6781−6786

compared to antibodies in regards of their affinity and specificity toward their targets as well as in their potential uses. An additional advantage of aptamers is that they can function under conditions that often cause antibodies to become irreversibly inactivated.[19]

Here we focus on another advantage of aptamers that is important in diagnostic applications, the ability to select high specificity variants by employing counter-selection to eliminate cross reactivity with closely related molecules. Examples of this specificity include discrimination between theophylline and caffeine despite the two molecules differing only by a methyl group,[20] an aptamer that enantioselectivly binds L-arginine over D-arginine,[21] and an aptamer that can distinguish between the human glioblastoma cell lines U87MG and T98G,[22] where they only differ by a mutation in p53. This distinctive feature led us to employ aptamers to achieve strain-specific discrimination in LFAs for influenza virus detection. Currently available LFAs based on antibodies against influenza virus may have type or subtype specificity depending on which antibodies have been chosen and what the assay is designed to achieve, for example, distinguishing influenza A from B.[23,24]

Aptamers, because of the nature of the SELEX (systematic evolution of ligand by exponential enrichment) process, can take advantage of counter-selection steps during their production and therefore can provide the required discrimination between strains. Aptamers showing discrimination between strains of a given subtype have been demonstrated where, for example, a RNA aptamer has been selected to bind to one H3N2 strain, A/Panama/2007/99, but not to other strains of the H3N2 subtype.[25] This RNA aptamer binds to virus envelope's most abundant protein, the hemagglutinin, H3, and is able to distinguish between the particular strain it selected for and other strains of the H3N2 subtype. This discrimination was achieved by counter-selection against whole virus particles of a closely related H3N2 strain during the SELEX process. The strain specificity of this aptamer was demonstrated using surface plasmon resonance with other H3N2 strains (A/Wyoming/3/2003, A/Sydney/05/97, and A/Wuhan/359/95),[25] but it has not previously been employed in LFAs to achieve strain-specific detection.

The rapid nature of LFAs for influenza virus detection is of great benefit for transmission control and prevention, as the viruses can spread in a variety of locales and in many cases are highly contagious through air and physical contact routes. LFAs as point-of-care devices have long been considered to be useful for the detection of viral infections.[26] Antibodies for influenza viruses can show different, and often broad, ranges of specificity.[27,28] This is likely due to the monoclonal antibodies arising from an immune response to the antigen of interest but without a counter-selection mechanism to allow discrimination against other strains.[29] Influenza viruses are known to acquire amino acid substitutions with great ease. These substitutions can lead to a significant difference in virulence, transmission, and/or mortality rate so that distinguishing between more and less virulent strains is important. An illustration of this is the 2009 influenza A (H1N1pdm09) "swine flu" pandemic strain that emerged to replace the classic seasonal flu, also a H1N1 subtype, and at one stage the two viruses were cocirculating.[30]

A LFA for detection of small molecules (adenosine and cocaine) that completely replaced antibodies by aptamers was first introduced by Lu et al.,[31,32] but since then only a handful of aptamer LFAs have been described.[33,34] One major drawback of using aptamers in LFAs is that the control line employed for assay assurance often yields a broad, indistinct shape, owing to the slow kinetics of target binding by immobilized aptamers.[35] It would be highly advantageous to combine the specificity of aptamers with the rapid surface binding kinetics of the streptavidin–biotin interaction,[36,37] and we have employed this combination in DRELFA (Figure 1).

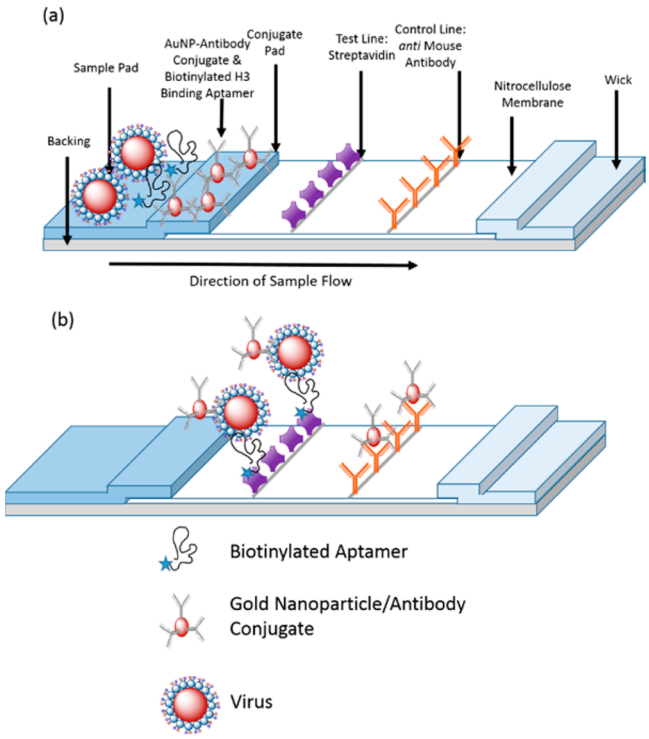

Figure 1. Schematic diagram of a DRELFA for detection of a virus. An anti-virus antibody (Y-shape) is conjugated with GNPs (golden oval). An aptamer (black line) has a biotin (blue star) at its 5′-or 3′-end. (a) In the presence of the specific virus, both the aptamer and the gold nanoparticle (GNP)-conjugated antibody bind to the virus (brown-textured sphere) and the biotin on the aptamer enables the complex to be bound onto the streptavidin test line (purple line) and the detection can be made by the color of GNPs. (b) Absence of the specific virus would result in the capture of GNPs on the secondary antibody control line (red line) only.

To illustrate a DRELFA that can detect a specific virus strain of interest, we paired a highly strain-specific aptamer with a biotin at either the 5′ or 3′ end with a less specific antibody labeled with gold nanoparticles (GNPs). The biotin-tagged aptamer is captured by streptavidin printed at the test line and this yields rapid capture kinetics. The excess of GNP-labeled monoclonal antibody is captured by a secondary antibody printed at the control line which also has fast kinetics. In the presence of the virus, both the aptamer and the monoclonal antibody bind to the virus to form a complex which is then captured by streptavidin through the biotinylated aptamer and shown by the color of the complexed antibody-GNPs conjugates on the test line. In the absence of virus, the complex is not formed and therefore no signal of GNPs is shown on the test line. This approach enables fast capture kinetics on both test and control lines and has been used in double antibody-based LFAs.[10]

DOI: 10.1021/acs.analchem.7b01149
Anal. Chem. 2017, 89, 6781–6786

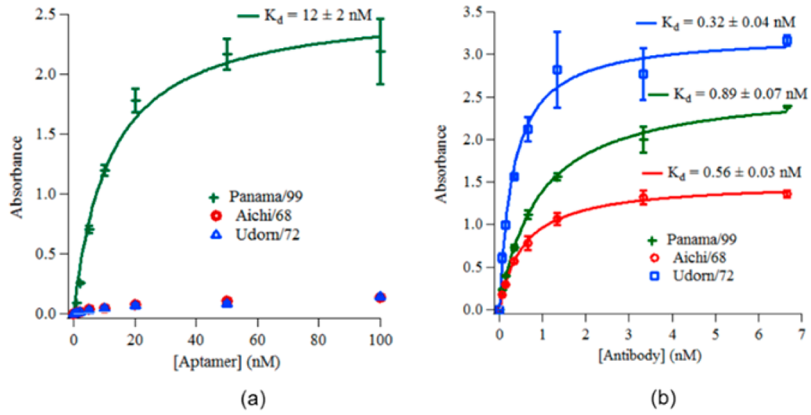

Figure 2. (a) Binding of an RNA aptamer to whole virus particles of 3 different strains of the influenza A H3N2 using ELONA: A/Panama/2007/99 (Panama/99), A/Aichi/2/68 (Aichi/68), and A/Udorn/307/72 (Udorn/72). The aptamer can discriminate one strain from others of the H3N2 subtype. (b) A monoclonal antibody shows binding to all three strains of the influenza A H3N2: Panama/99, Aichi/68, and Udorn/72. In all cases 7 × 10^8 virus particles were added to each well for immobilization of the virus on the microtiter plate.

MATERIALS AND METHODS

Materials and Reagents. All the oligonucleotides were synthesized and HPLC purified by Integrated DNA Technologies. and the sequences are listed in the Supporting Information,SI Table. Anti-hemagglutinin H3 antibody (ab82454), anti-hemagglutinin H5 antibody (ab82455), and goat anti-mouse antibody (ab6708) were from Abcam. Anti-hemagglutinin H7 antibody (ABIN573415) from Antibodies-Online and anti-hemagglutinin H9 antibody (ID, 955HA9) was produced at the Pirbright Institute (U.K.).[38] HAuCl4 was purchased from Sigma. HiFlow Pus membrane, glass fiber conjugate sheet, and cellulose fiber roll were from Merck Millipore. Other common reagents were bought from Sigma unless specified.

Methods. *Preparation of the RNA Aptamers.* The ssDNA template sequence for the A/Panama/2007/99 (H3N2) was TCTAA TACGA CTCAC TATAG GGAGA ATTCC GACCA GAAGG GTTAG CAGTC GGCAT GCGGT ACAGA CAGAC CTTTC CTCTC TCCTT CCTCT TCT (underlined for T7 promoter). This ssDNA template was then amplified using a forward primer (H3P07) TCTAA TACGA CTCAC TATAG GGAGA ATTCC GACCA GAAG and a reverse primer (RevH3P07), OneTaq DNA polymerase (New England Biolabs), and the dNTP mix (Promega) to generate and amplify dsDNA. The obtained dsDNA was purified by ethanol precipitation and transcribed into the RNA using an AmpliScribe T7-Flash transcription kit from Epicenter. The RNA obtained from the transcription was then purified using 10% polyacrylamide TBE-urea gel electrophoresis. The RNA sequence obtained (GGGAG AAUUC CGACC AGAAG GGUUA GCAGU CGGCA UGCGG UACAG ACAGA CCUUU CCUCU CUCCU UCCUC UUCU), the RNA aptamer for the A/Panama/2007/99 (H3N2) (RNAH3-P07Apt), was hybridized with excess DNA biotin linker (ApH3P07Linker, 5′-biotin-TEG- AGAAGAGGAAGGAGA-GAGG) with a molar ratio of RNA aptamer−DNA biotin linker = 1:1.2 to add a biotin on the RNA aptamer 3′-end. The excess amount of DNA biotin linker was removed using 10 kDa Amicon centrifugal filters (Millipore) prior to being used in the DRELFA.

For other aptamers, their sequences and the corresponding ssDNA templates and the primer pairs used for PCR were specified in SI Table in the Supporting Information.

Synthesis of Gold Nanoparticles (GNPs). GNPs were synthesized by the sodium citrate method.[39] GNPs were synthesized in a 50 mL batch using a 100 mL glass flash bottle with a glass-coated stir bar. First, 49 mL of deionized ultrafiltered water was poured into the flash bottle with the stir bar, and then 1 mL of freshly made 12.7 mM chloroauric acid solution was added. The bottle was placed on a magnetic stirrer hot plate (200 °C, 150 rpm) and brought to boiling. A variable volume of 38.8 mM of trisodium citrate solution was added, and the solution was kept at boiling for a further 10 min. It was then cooled down to room temperature with stirring (100 rpm). Volumes of 0.8 mL for GNPs with nominal diameters of 25 nm, 0.5 mL for GNPs of 40 nm, and 0.4 mL for GNPs of 60 nm were used. The diameters were then determined experimentally using Nanoparticle Tracking Analysis (NTA) and gave values of 37, 55, and 72 nm, respectively.

Conjugation of Antibodies to GNPs. Antibodies were transferred to 2 mM borax buffer (pH 9.0) using the Zebra spin desalting column (7 kDa MWCO) from ThermoFisher. Suitable volumes of a borax stock solution (500 mM, pH 9.0) to a final concentration of 2 mM were added to the freshly made GNPs. Anti-hemagglutinin H3 antibody and anti-hemagglutinin H5 antibody were conjugated with the 37 nm GNPs, anti-hemagglutinin H7 antibody was conjugated with the 55 nm GNPs, and anti-hemagglutinin H9 antibody was conjugated with the 72 nm GNPs. Antibody stock solutions were added to a final concentration of 5 μg/mL in a solution of GNPs having an o.d. of 1 at the wavelength of maximum absorbance. The solutions were placed on a tube rotator at room temperature for 4 h and then in a cold room (4 °C) overnight. Finally, 5% BSA in 2 mM borax (pH 9.0) was added to give a final concentration of 0.5% BSA and rotated at room temperature for 30 min. The antibody-GNP conjugates were then washed 3 times using centrifugation with buffer (0.5% BSA, 4% sucrose, 0.02% Tween20 in 20 mM HEPES, pH 7.3).

Preparation of the Lateral Flow Test Strips. A lateral flow strip was assembled from 3 parts (bottom up): a glass fiber conjugate pad (26 mm), HiFlow Plus membrane (25 mm), and wicking pad (15 mm). Before assembling, the HiFlow Plus membrane was printed with a test line and a control line and the conjugate pad was treated as described below.

DOI: 10.1021/acs.analchem.7b01149
Anal. Chem. 2017, 89, 6781−6786

Figure 3. Specificity of LFA's (a) DRELFA: The sample with Panama/99 has 2 lines showing visual detection of this virus strain while measurements for Udorn/72 and Aichi/68 samples have only 1 line (control quality) indicating that this DRELFA for Panama/99 virus does not have any cross reactivity with other strains of this H3N2 subtype. (b) Antibody-LFA: all 3 samples of the influenza A H3N2 displayed 2 lines showing visual detection of the viruses, indicating that the conventional LFA does not differentiate between the three virus strains of the H3N2 subtype. The measurements were performed with samples of 10^8 virus particles. The sample volume was 100 μL.

Conjugate Pad Treatment. Conjugate pads were dipped into a solution containing 1% BSA, 0.2% Tween20, 4% sucrose in 20 mM HEPES, pH 7.3 for 30 min. The pads were then taken out and left to dry overnight.

Printing of Test and Control Lines. The membrane was printed with a streptavidin test line and an anti-mouse antibody control line using a Scienion sciFLEXARRAYER S3 with a type 4 piezo. The test line consisted of 10 lines of 50 μm pitch and were printed at a speed of 0.1 μL/cm of 2 mg/mL streptavidin in 10 mM acetate buffer pH 5.0. The control line consisted of 5 lines of 100 μm pitch printed with 0.1 μL/cm of 1 mg/mL of goat anti-mouse antibody in 10 mM borax buffer pH 8.5.

Assembling the Strip. The HiFlow Plus membrane of 25 mm width was already placed on a 60 mm adhesive plastic backing card. The HiFlow Plus membrane is cellulose ester with a nominal capillary flow of 180 s/4 cm. Conjugate pads were cut from a Millipore glass fiber sheet with a width of 26 mm and the wicking pads were cut from Millipore cellulose fiber sheet to bands with a width of 15 mm. The conjugate pads and the wicking pads were attached to the HiFlow Plus membrane card with a 2 mm overlap between pads. The assembled card was then placed between 2 clean plastic sheets and pressed lightly with a roller. The assembled card was cut to 5 mm wide strips using a Fellowes Astro Cutter. The strips were then housed in plastic cassettes and stored in an amber tinted desiccator cabinet with humidity around 20%.

Lateral Flow Assay. The assay was run with 100 μL samples (in 20 mM Hepes, 0.1% Triton X-100, pH 7.4). Typically, the time between adding the samples and recording the images was 15 min. The images were taken with a digital camera.

RESULTS AND DISCUSSION

Influenza Virus Strain Specificity of the Aptamer. Enzyme linked oligonucleotide assay (ELONA) data shown in Figure 2a confirms that aptamers with a high level of discrimination can be specifically selected for the A/Panama/2007/99 strain of H3N2 virus over other H3N2 strains by suitable choice of counter-selection regimes.[25] A commercially available anti-H3 HA monoclonal antibody, on the other hand, binds all of the three tested strains of the H3N2 subtype as shown in Figure 2b. We aim to transfer this high specificity of aptamers into a LFA diagnostic platform using a format we call dual recognition element lateral flow assay (DRELFA).

Strain-Specific Detection of Influenza Virus Using DRELFA. To demonstrate strain-specific detection in the proposed format, a DRELFA was built from paring a Panama/99-specific RNA aptamer[25] having a biotin at its 5′-end[40] with an anti-H3 antibody conjugated with 37 nm GNPs. As shown in Figure 3a this DRELFA detected the Panama/99 strain without any observable cross-reactivity with two other strains of the H3N2 subtype, Aichi/68 and Udorn/72. On the other hand, as shown in Figure 3b, a conventional antibody-based LFA with these virus strains show cross-reactivity between the different strains of this subtype. Conventional LFA systems built from different antibodies would show different results depending on how broad a cross-reactivity they exhibit.

Furthermore, the DRELFA system were also used to assess nonspecific binding with three different viruses (Newcastle disease virus (NDV) and infectious bronchitis virus (IVB) that cause common viral respiratory diseases and an influenza B virus (Florida/04/2006). As shown in the Supporting Information, SI1 Figure, the DRELFA demonstrated that even for samples of high concentrations of virus particles, 100% specificity with no visually detectable signal against any of these three viruses. This is probably due to the aptamer produced with counter-selection for high specificity can also reduce nonspecific binding. Finally, the production of DRELFA strips can be readily adapted to a wide range of targets as the test line is always streptavidin and the control line is always a secondary antibody.

To assess the distribution of virus particles on the DRELFA strips they were analyzed using quantitative real time-PCR (qRT-PCR). Four different regions of the LF membrane were taken: before the test line, the test line, between the test and control lines, and the control line. RNA was extracted from these regions, and a probe for the M gene was used to reverse transcribe it into cDNA for quantitation by qRT-PCR as described by Londt et al.[41] The corresponding virus copies of the extracted regions of the samples are shown in Figure 4a.

DOI: 10.1021/acs.analchem.7b01149
Anal. Chem. 2017, 89, 6781−6786

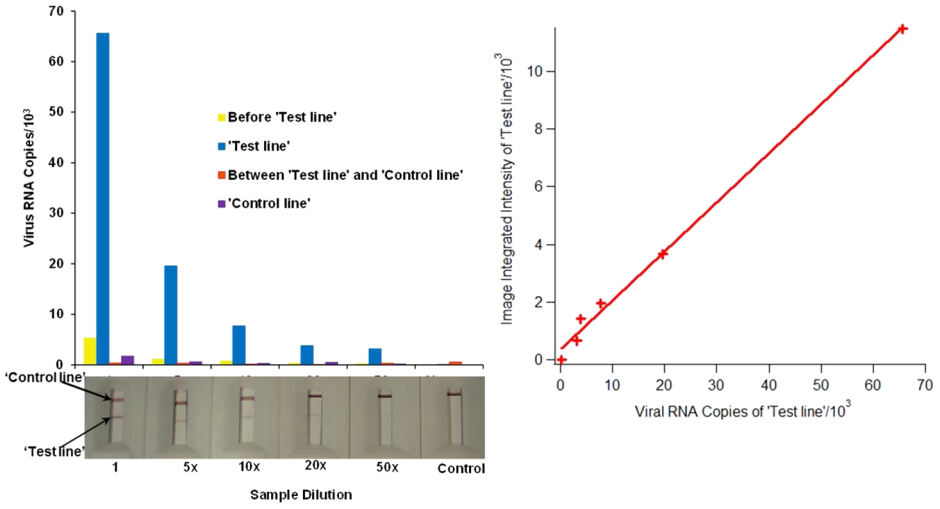

(a) (b)

Figure 4. (a) Distribution of the virus particles on the lateral flow membranes were analyzed using qRT-PCR. It shows that consistently >90% of the virus particles are captured on the test line. (b) Comparison of the intensity of the test lines' signals to the virus copies obtained from the RNA using qRT-PCR at different virus dilutions. The image intensity and the RNA copy number have a correlation coefficient of 0.995.

Table 1. Detection of Viruses Using DRELFAs

virus strain	H3N2 DRELFA[a]	H5N1 DRELFA[b]	H9N2 DRELFA[c]
A/Panama/2007/99 (H3N2)	+	–	–
A/Aichi/2/68 (H3N2)	–	–	–
A/Udorn/307/72 (H3N2)	–	–	–
A/Vietnam/1203/2004 (H5N1)	–	+	–
A/turkey/Turkey/1/2005 (H5N1)	–	+	–
A/turkey/Italy/1279/99 (H7N1)[d]	–	+	–
A/chicken/Pakistan/UDL/2008 (H9N2)	–	+	+

[a]Pairing an RNA aptamer for Panama/99 (H3N2) and an anti H3 antibody. [b]Paring an RNA aptamer for H5N1 and an anti H5 (*H7) antibody. [c]Pairing a DNA aptamer for H9N2 and an anti H9 antibody. [d]See the Supporting Information, SI3 Figure 1,2.

The blue bars represent the number of copies of viral RNA at each location indicating that the great majority (consistently over 90%) of the viral RNA is at the test line. This confirmed that DRELFA is very effective in localizing the analyte to the test line and this is crucial for the sensitivity of the device.

The color of the test line is visible down to 50-fold dilution, equivalent to 2×10^6 virus particles. The typical influenza virus viral load range 10^9 to 10^3 copies/mL in respiratory samples depending on the time when the samples were taken and the virus strains.[42−44] The DRELFA can therefore detect the samples taken in the early days of the symptoms (where the viral loads are higher). We also used simple image analysis to compare the color intensities of the visible test lines with the number of virus RNA copies obtained from the qRT-PCR. Figure 4b shows a very good correlation between the two, indicating consistency between the qRT-PCR results and visual signals.

Choice of Aptamers and the Specificity of DRELFAs. The specificity of DRELFAs depends on the specificity of the aptamer employed. As shown in Figure 1, strain-specific aptamers can be used; however, aptamers can also be made for a broader range of influenza viruses (e.g., the H5N1 and H7N1 subtypes)[45,46] depending on how the selections and counter selections are designed. We performed ELONA binding assays on an aptamer with cross-subtype binding, and the data are shown in the Supporting Information SI2 Figure. The DRELFAs are based on aptamers with different levels of specificity such as strain-specific binding to influenza A/Panama/2007/99 and more general for subtypes H5N, H7N1, and H9N2. Using the same type of DRELFA strips that have test lines printed with streptavidin and the control lines printed with a secondary antibody, we also have prepared DRELFA devices to detect virus strains of other subtypes as shown in the Table 1 and in the Supporting Information, SI3 Figure 1,2.

■ CONCLUSION

We have demonstrated that pairing an aptamer and an antibody in a DRELFA format offers direct detection of whole virus particles with high specificity, thereby allowing discrimination of a specific influenza strain (A/H3N2/Panama/2007/99) as a model target. The assay had a detection limit of 2×10^6 virus particles. DRELFA also showed no detectable signal for with neither NDV and IBV (common respiratory viruses) nor with an influenza B virus. Using quantitative real-time PCR (qRT-PCR), we showed that the DRELFA is very effective in capturing the analyte at the test line (capture efficiencies consistently over 90%), which is crucial for the sensitivity of the device. In addition, color intensities of the test lines in DRELFA showed a good correlation with qRT-PCR over a concentration range of 50-fold. Finally a lateral flow format that combinines a biotinylated aptamer with a streptavidin test line and a secondary antibody control line, as with double antibody LFAs, avoids the need to optimize the deposition of different capture antibodies.

DOI: 10.1021/acs.analchem.7b01149
Anal. Chem. 2017, 89, 6781−6786

■ ASSOCIATED CONTENT

Supporting Information

The Supporting Information is available free of charge on the ACS Publications Web site. SI Table for . The Supporting Information is available free of charge on the ACS Publications website at DOI: 10.1021/acs.analchem.7b01149.

Oligonucleotide sequences, cross-reactivity test of DRELFA, specificity of aptamers, and other influenza virus subtypes' DRELFA (PDF)

■ AUTHOR INFORMATION

Corresponding Author

*E-mail: t.cass@imperial.ac.uk. Phone: +44-20-7594-5195.

ORCID

Anthony E. G. Cass: 0000-0001-8881-4786

Author Contributions

All authors have given approval to the final version of the manuscript.

Notes

The authors declare no competing financial interest.

■ ACKNOWLEDGMENTS

The work was supported by BBSRC ZELS Grant BB/L018853/1. J.W.M. and D.J.B. were supported by the Francis Crick Institute and receive their core funding from Cancer Research UK (Grant FC001030), the UK Medical Research Council (Grant FC001030), and the Wellcome Trust (Grant FC001030). The authors would like to thank Dr. Christopher Johnson for taking photos of the LFA devices and Ms. Rachel Sim for helping with the drawing of Figure 2.

■ REFERENCES

(1) Taubenberger, J.; Morens, M. D. *Emerging Infect. Dis.* **2006**, *12*, 15.

(2) Kilbourne, D. E. *Emerging Infect. Dis.* **2006**, *12*, 9.

(3) World Health Organization. In *Implement of the International Health Regulations 2005*; 64th World Health Assembly, 2011.

(4) World Organisation for Animal Health. *Update on Highly Pathogenic Avian Influenza in Animals (Type H5 and H7)*, http://www.oie.int/animal-health-in-the-world/update-on-avian-influenza/2016/.

(5) Food and Agricultural Organization of the United Nations. *Avian Influenza*, http://www.fao.org/avianflu/en/index.html.

(6) WHO. *Cumulative number of confirmed human cases for avian influenza A(H5N1) reported to WHO, 2003–2017*, http://www.who.int/influenza/human_animal_interface/2017_01_16_tableH5N1.pdf?ua=1.

(7) Boivin, G.; Côté, S.; Déry, P.; De Serres, G.; Bergeron, M. G. *J. Clin. Microbiol.* **2004**, *42*, 45–51.

(8) Chen, W.; He, B.; Li, C.; Zhang, X.; Wu, W.; Yin, X.; Fan, B.; Fan, X.; Wang, J. *J. Med. Microbiol.* **2007**, *56*, 603–7.

(9) Pai, N. P.; Vadnais, C.; Denkinger, C.; Engel, N.; Pai, M. *PLoS Med.* **2012**, *9*, e1001306.

(10) Wong, R. C.; Tse, H. Y. *Lateral Flow Immunoassay*; Springer: New York, 2009.

(11) Li, J.; Macdonald, J. *Biosens. Bioelectron.* **2016**, *83*, 177–192.

(12) Rissin, D. M.; Kan, C. W.; Campbell, T. G.; Howes, S. C.; Fournier, D. R.; Song, L.; Piech, T.; Patel, P. P.; Chang, L.; Rivnak, A. J.; Ferrell, E. P.; Randall, J. D.; Provuncher, G. K.; Walt, D. R.; Duffy, D. C. *Nat. Biotechnol.* **2010**, *28*, 595–599.

(13) Lee, B. W.; Bey, R. F.; Baarsch, M. J.; Simonson, R. R. *J. Vet. Diagn. Invest.* **1993**, *5*, 510–515.

(14) Haarburger, D.; Pillay, T. S. *J. Clin. Pathol.* **2011**, *64*, 546–548.

(15) Ellington, A. D.; Szostak, J. W. *Nature* **1990**, *346*, 818–822.

(16) Tuerk, C.; Gold, L. *Science* **1990**, *249*, 505–10.

(17) Cho, E. J.; Lee, J.-W.; Ellington, A. D. *Annu. Rev. Anal. Chem.* **2009**, *2*, 241–264.

(18) Keefe, A. D.; Pai, S.; Ellington, A. *Nat. Rev. Drug Discovery* **2010**, *9*, 660–660.

(19) Jayasena, S. D. *Clin. Chem.* **1999**, *45*, 1628–1650.

(20) Jenison, R.; Gill, S.; Pardi, A.; Polisky, B. *Science* **1994**, *263*, 1425–1429.

(21) Geiger, A.; Burgstaller, P.; von der Eltz, H.; Roeder, A.; Famulok, M. *Nucleic Acids Res.* **1996**, *24*, 1029–1036.

(22) Cerchia, L.; Esposito, C. L.; Jacobs, A. H.; Tavitian, B.; de Franciscis, V. *PLoS One* **2009**, *4*, e7971.

(23) Cazacu, A. C.; Chung, S. E.; Greer, J.; Demmler, G. J. *J. Clin. Microbiol.* **2004**, *42*, 3707–3710.

(24) Leonardi, G. P.; Wilson, A. M.; Zuretti, A. R. *J. Virol. Methods* **2013**, *189*, 379–82.

(25) Gopinath, S. C. B.; Misono, T. S.; Kawasaki, K.; Mizuno, T.; Imai, M.; Odagiri, T.; Kumar, P. K. R. *J. Gen. Virol.* **2006**, *87*, 479–487.

(26) Oem, J. K.; Ferris, N. P.; Lee, K.-N.; Joo, Y.-S.; Hyun, B.-H.; Park, J.-H. *Clinical and Vaccine Immunology* **2009**, *16*, 1660–1664.

(27) Burlington, D. B.; Wright, P. F.; van Wyke, K. L.; Phelan, M. A.; Mayner, R. E.; Murphy, B. R. *J. Clin. Microbiol.* **1985**, *21*, 847–849.

(28) Wang, M. L.; Skehel, J. J.; Wiley, D. C. *J. Virol.* **1986**, *57*, 124–128.

(29) Goding, J. W. *Monoclonal Antibodies: Principles and Practice*; Academic Press: London, U.K., 1996.

(30) Tscherne, D. M.; García-Sastre, A. *J. Clin. Invest.* **2011**, *121*, 6–13.

(31) Liu, J.; Mazumdar, D.; Lu, Y. *Angew. Chem., Int. Ed.* **2006**, *45*, 7955–7959.

(32) Liu, G.; Mao, X.; Phillips, J. A.; Xu, H.; Tan, W.; Zeng, L. *Anal. Chem.* **2009**, *81*, 10013–10018.

(33) Chen, A.; Yang, S. *Biosens. Bioelectron.* **2015**, *71*, 230–242.

(34) Jauset-Rubio, M.; Svobodová, M.; Mairal, T.; McNeil, C.; Keegan, N.; El-Shahawi, M. S.; Bashammakh, A. S.; Alyoubi, A. O.; O'Sullivan, C. K. *Anal. Chem.* **2016**, *88*, 10701–10709.

(35) Bruno, J. G.; Carrillo, M. P.; Richarte, A. M.; Phillips, T.; Andrews, C.; Lee, J. S. *BMC Res. Notes* **2012**, *5*, 633.

(36) Duan, X.; Li, Y.; Rajan, N. K.; Routenberg, D. A.; Modis, Y.; Reed, M. A. *Nat. Nanotechnol.* **2012**, *7*, 401–407.

(37) Pierres, A.; Touchard, D.; Benoliel, A.-M.; Bongrand, P. *Biophys. J.* **2002**, *82*, 3214–3223.

(38) Peacock, T.; Reddy, K.; James, J.; Adamiak, B.; Barclay, W.; Shelton, H.; Iqbal, M. *Sci. Rep.* **2016**, *6*, 18745.

(39) Frens, G. *Nature, Phys. Sci.* **1973**, *241*, 20–22.

(40) Le, T. T.; Adamiak, B.; Benton, D. J.; Johnson, C. J.; Sharma, S.; Fenton, R.; McCauley, J. W.; Iqbal, M.; Cass, A. E. G. *Chem. Commun.* **2014**, *50*, 15533–15536.

(41) Löndt, B. Z.; Nunez, A.; Banks, J.; Nili, H.; Johnson, L. K.; Alexander, D. J. *Avian Pathol.* **2008**, *37*, 619–627.

(42) Ngaosuwankul, N.; Noisumdaeng, P.; Komolsiri, P.; Pooruk, P.; Chokephaibulkit, K.; Chotpitayasunondh, T.; Sangsajja, C.; Chuchottaworn, C.; Farrar, J.; Puthavathana, P. *Virol. J.* **2010**, *7*, 75–75.

(43) To, K. K. W.; Chan, K.-H.; Li, I. W. S.; Tsang, T.-Y.; Tse, H.; Chan, J. F. W.; Hung, I. F. N.; Lai, S.-T.; Leung, C.-W.; Kwan, Y.-W.; Lau, Y.-L.; Ng, T.-K.; Cheng, V. C. C.; Peiris, J. S. M.; Yuen, K.-Y. *J. Med. Virol.* **2010**, *82*, 1–7.

(44) Lee, N.; Chan, P. K. S.; Hui, D. S. C.; Rainer, T. H.; Wong, E.; Choi, K.-W.; Lui, G. C. Y.; Wong, B. C. K.; Wong, R. Y. K.; Lam, W.-Y.; Chu, I. M. T.; Lai, R. W. M.; Cockram, C. S.; Sung, J. J. Y. *J. Infect. Dis.* **2009**, *200*, 492–500.

(45) Gopinath, S. C. B.; Kumar, P. K. R. *Acta Biomater.* **2013**, *9*, 8932–8941.

(46) Suenaga, E.; Kumar, P. K. R. *Acta Biomater.* **2014**, *10*, 1314–1323.

DOI: 10.1021/acs.analchem.7b01149
Anal. Chem. 2017, 89, 6781–6786